



ISSN: 2321-9114

AJEONP 2019; 7(2): 23-29

© 2019 AkiNik Publications

Received: 14-02-2019

Accepted: 16-03-2019

**Larissa M de Oliveira**

Laboratório de Polímeros Nanoestruturados (NANOPOL), Universidade Federal do Amazonas (UFAM), Manaus/AM, Brasil

**Suzan X Lima**

a) Laboratório de Polímeros Nanoestruturados (NANOPOL), Universidade Federal do Amazonas (UFAM), Manaus/AM, Brasil  
 b) Programa de Pós-graduação em Ciência e Engenharia de Materiais (PPGCEM), Universidade Federal do Amazonas (UFAM), Manaus/AM, Brasil

**Laiane S da Silva**

a) Laboratório de Polímeros Nanoestruturados (NANOPOL), Universidade Federal do Amazonas (UFAM), Manaus/AM, Brasil  
 b) Programa de Pós-graduação em Ciência e Engenharia de Materiais (PPGCEM), Universidade Federal do Amazonas (UFAM), Manaus/AM, Brasil

**Josiana M Mar**

a) Laboratório de Polímeros Nanoestruturados (NANOPOL), Universidade Federal do Amazonas (UFAM), Manaus/AM, Brasil  
 b) Programa de Pós-graduação em Ciência e Engenharia de Materiais (PPGCEM), Universidade Federal do Amazonas (UFAM), Manaus/AM, Brasil

**Sidney G Azevedo**

Laboratório de Polímeros Nanoestruturados (NANOPOL), Universidade Federal do Amazonas (UFAM), Manaus/AM, Brasil

**Maxwaldo S Rabelo**

Laboratório de Polímeros Nanoestruturados (NANOPOL), Universidade Federal do Amazonas (UFAM), Manaus/AM, Brasil

**Henrique D da Fonseca Filho**

a) Laboratório de Polímeros Nanoestruturados (NANOPOL), Universidade Federal do Amazonas (UFAM), Manaus/AM, Brasil  
 b) Departamento de Física, Universidade Federal do Amazonas (UFAM), Manaus/AM, Brasil

**Pedro H Campelo**

a) Laboratório de Polímeros Nanoestruturados (NANOPOL), Universidade Federal do Amazonas (UFAM), Manaus/AM, Brasil  
 b) Programa de Pós-graduação em Ciência e Engenharia de Materiais (PPGCEM), Universidade Federal do Amazonas (UFAM), Manaus/AM, Brasil

**Edgar A Sanches**

a) Laboratório de Polímeros Nanoestruturados (NANOPOL), Universidade Federal do Amazonas (UFAM), Manaus/AM, Brasil  
 b) Programa de Pós-graduação em Ciência e Engenharia de Materiais (PPGCEM), Universidade Federal do Amazonas (UFAM), Manaus/AM, Brasil  
 c) Departamento de Física, Universidade Federal do Amazonas (UFAM), Manaus/AM, Brasil

**Correspondence:****Larissa M de Oliveira**

Laboratório de Polímeros Nanoestruturados (NANOPOL), Universidade Federal do Amazonas (UFAM), Manaus/AM, Brasil

## Controlled release of *Licaria puchury-major* essential oil encapsulated in PCL/gelatin-based colloidal systems and membranes

**Larissa M de Oliveira, Suzan X Lima, Laiane S da Silva, Josiana M Mar, Sidney G Azevedo, Maxwaldo S Rabelo, Henrique D da Fonseca Filho, Pedro H Campelo and Edgar A Sanches**

**Abstract**

Different concentrations of the essential oil (EO) from *Licaria puchury-major* (Lauraceae) was encapsulated in polycaprolactone (PCL)/gelatin wall materials in the colloid systems form. PCL/gelatin-based colloid systems were prepared using the coacervation method with encapsulation efficiency higher than 90%. The colloid form containing 500 µg mL<sup>-1</sup> of EO was freeze-dried to form membrane-based micro particles. Then, the EO controlled release from all samples was evaluated. The loaded and unloaded nanoparticles were spherical and dependent on the EO concentration, with average size estimated to be 60–310 nm. The zeta potential technique indicated a stable colloidal system. The FTIR spectra of the colloidal systems and membrane confirmed the successful encapsulation of EO within the wall materials. The membrane images revealed that the lyophilization process promoted an agglomeration of nanoparticles, resulting in particles in micrometric sizes. All colloidal systems released their EO up to 100 h. The EO release from membrane was faster than that observed for the colloidal systems. The Korsmeyer-Peppas model better adjusted the controlled release data of the colloidal systems confirming the anomalous or non-Fickian type diffusion mechanism. The same model also better adjusted the controlled release data of the membrane system with  $n > 0.5$ . The EO from *L. puchury-major* could be encapsulated successfully within the developed PCL/gelatin particles. The developed colloidal systems or membrane-based gelatin particles containing this EO was shown to be feasible as a sustainable alternative as a natural bio-defensive due to their encapsulation efficiency, biodegradability and abundance of this plant in the Amazon region.

**Keywords:** *Licaria puchury-major*, PCL/gelatin-based nanoparticles, controlled release, essential oil

**1. Introduction**

Natural controlling agents have long been considered as acceptable alternatives for pest management [1–6]. The encapsulation of essential oils (EO) in controlled release formulations can improve their physicochemical properties and bioavailability/efficiency, while reducing the required concentrations and environmental damages [7–9]. The controlled release of EO encapsulated in biopolymeric nanoparticles is of special interest due to the prolonged duration of action, and the biological degradation of wall materials [10]. For this reason, PCL and gelatin nanoparticles have been employed successfully as a carrier for drugs and bioactive molecules [7, 11–13]. *Licaria puchury-major* (Mart.) Kosterm. (Lauraceae) (known in Brazil as puxuri, puchury or pixuri) is native from Amazon and has been often used in the Brazilian northern folk medicine for stomach and intestinal diseases, as well as to treat insomnia and irritability [10–12]. Previous work reported the bioactivity and the lethal dosages of this essential oil against *Tetranychus urticae* Koch., *Cerataphis lataniae* Boisd. and *Aedes aegypti* Linn. [4]. The sepests are currently causing severe damage to human health, as well as to open-field and protected crops [14–16]. Considering the previous reported effectiveness of this EO to control the tested pests, the aim of this paper was to develop biodegradable nano-particles in the forms of colloidal system and membranes, as well as evaluate the controlled release and of this EO. This EO was encapsulated in different concentrations to form colloidal systems. Then, the colloidal system containing the higher concentration of OE was freeze-dried to form a membrane-based PCL/gelatin microparticles. Studies reporting the encapsulation of the *L. puchury-major* EO to be used in controlled-release formulations have not been reported in the scientific literature. On the other hand, the freeze-dried colloidal system to form membranes

could represent an alternative and efficient tool to develop new controlled-release materials. Keeping in mind the search for possible sustainable control tools based on the prolonged effect of natural bioactive substances, the present paper may be useful to stimulate the development of a new effective controlling agents based on PCL/gelatin biodegradable particles.

## 2. Materials and Methods

### 2.1. Essential Oil Acquisition

Seeds of *L. Puchury-major* were collected in Belém/PA–Brazil (Sis Gen n° A26CD5E). The botanical identification was carried out at the Federal University of Amazonas (UFAM). A portion of 150 g of powdered seeds was subjected to hydro distillation using a Clevenger-type apparatus for 3 h at 100 °C.

### 2.2. Colloidal System and Membrane-based PCL/Gelatin microparticles

Gelatin type B was heated to 50°C in distilled water under constant stirring. Then, tween 80 was solubilized at 40°C (Solution I). The Solution II was prepared using polycaprolactone (PCL, 0.05 g), span 60 (0.02 g) and caprylic/capric triglyceride acid (TACC, 0.1 g) solubilized in dichloromethane (5 mL). The EO was added to the Solution II. After solubilization, the Solution II was added to Solution I using an ultra-disperser (10,000 rpm). Then, transglutaminase was added to the final solution, which was maintained at constant stirring (25 °C) until total solvent evaporation. Samples were labeled as follow: PUC<sub>100</sub>, PUC<sub>250</sub> and PUC<sub>500</sub> (systems containing absolute concentrations of 100 µg mL<sup>-1</sup>, 250 µg mL<sup>-1</sup> and 500 µg mL<sup>-1</sup> of EO, respectively). Then, the sample PUC<sub>500</sub> was maintained for 48 h at -18°C and freeze-dried for 10 h at -40°C in a Terroni Enterprise freeze-drier to obtain the PCL/gelatin-based microparticles in the membrane form (labeled as PUCM<sub>500</sub>).

### 2.3. FTIR Measurement

A Bomem MB Series Hartmann & Braun spectrophotometer was used to evaluate the molecular stretching of the *in natura* EO, the unloaded nanoparticles, the nanoparticles loaded with EO and the membrane-based PCL/gelatin microparticles. The wave number was in the range of 4,000 to 500 cm<sup>-1</sup> using 32 scans.

### 2.4. Atomic Force Microscopy (AFM) and Scanning Electron Microscopy (SEM)

Topographies of the gelatin-based nanoparticles in the form of colloidal systems were obtained with an AFM (Innova, Bruker) on an area of (10×10) µm<sup>2</sup>, operated in contact mode using silicon nitride cantilevers. Samples were deposited in a glass plate until solvent evaporation. Measurements were performed at 296 ± 1 K and 40 ± 1% R.H. with 512 × 512 pixels at a scan rate of 1.0 Hz. Particle size distribution was estimated using the Image J. program<sup>[17]</sup>. SEM images of the membrane-based gelatin microparticles (PUCM<sub>500</sub>) were obtained using a Supra 35, Carl Zeiss, 1kV. Membrane was deposited on a carbon tape and recovered with a thin gold layer. The surface morphology was evaluated at room temperature.

### 2.5. Zeta Potential

The zeta potential values (in mV) of the gelatin-based nanoparticles in the form of colloidal systems were determined using a Zetasizer Nano ZS90 instrument (Malvern

Instruments, UK). Samples (unloaded and loaded nanoparticles containing the absolute concentration of 500 µg mL<sup>-1</sup> of EO) were analyzed in triplicate, at 25°C.

### 2.6. Encapsulation Efficiency

The Encapsulation Efficiency (EE) of the EO within the gelatin-based nanoparticles in the form of colloidal systems was analyzed using UV-vis spectroscopy based on previous work<sup>[12]</sup> with some modifications. Nanoparticles were separated by centrifugation (20,000 rpm) and the supernatant absorbance was used to determine the amount of free EO. The EE was calculated using the formula: % EE = (Amount of encapsulated EO/absolute concentration of EO used in the formulation) × 100.

### 2.7. In vitro Essential Oil Release

The EO release was evaluated *in vitro* for the colloidal systems and membrane-based gelatin microparticles. The EO release from the colloidal systems was carried out using a dialysis tubing cellulose membrane suspended in water at 25°C. A portion of 2 mL was withdrawn at regular time intervals and their absorbance was measured using an UV-vis spectrophotometer. The amount of EO released was quantified using the standard curve according to a previous report<sup>[11]</sup>. The experiments were carried out in triplicate. The EO released from the membrane microparticles was carried out using a portion of 1.15 g of the sample PUCM<sub>500</sub> placed in 30 mL of distilled water. Then, 2 mL of solution was withdrawn at regular time intervals and the absorbance was measured using an UV-vis spectrophotometer.

## 3. Results & Discussion

### 3.1. FTIR and Encapsulation Efficiency

Figure 1 shows the FTIR spectra of the *in natura* EO of *L. puchury-major* (black curve), colloidal system containing unloaded nanoparticles (blue curve), colloidal system containing nanoparticles loaded with EO (red curve) and membrane-based PCL/gelatin microparticles (gray curve).

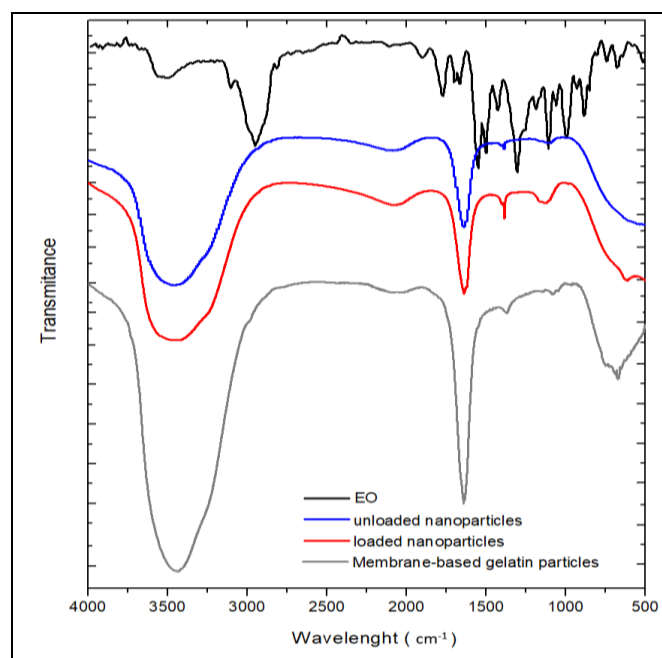


**Fig 1:** FTIR spectra of the *in natura* EO of *L. Puchury-major* (black curve), colloidal system containing unloaded nanoparticles (blue curve), colloidal system containing nanoparticles loaded with EO (red curve) and membrane-based gelatin particles (gray curve).

Safrole was identified as the major compound of this EO [4]. The main bands of safrole were assigned to the C=C stretching around  $1,663\text{ cm}^{-1}$  and olefinic C-H bending vibrations of a vinyl double bond around  $929\text{ cm}^{-1}$ . The band at  $1,040\text{ cm}^{-1}$  represents the C-O-C stretching. The antisymmetric and symmetric C-O stretching was observed, respectively, around  $989$  and  $1,184\text{ cm}^{-1}$ [18]. The blue curve shows the FTIR spectra of the colloidal unloaded nanoparticles. The observed bands are assigned to the nanoparticle's wall material [19]: the peak at approximately  $1,630\text{ cm}^{-1}$  was assigned to the amino group I (C=O and C-N stretch), while amino group II (mainly N-H bond) was verified at  $1,390\text{ cm}^{-1}$ . The absorption of the amino group III at  $1,140\text{ cm}^{-1}$  is attributed to the planar N-H bond. The red curve represents the spectrum of the colloidal nanoparticles loaded with EO and the gray curve shows the spectrum of the membrane-based PCL/gelatin microparticles loaded with EO. Both spectra presented similar characteristic absorption peaks when they were compared to the spectrum of the colloidal system containing unloaded nanoparticles. No prominent peaks related to the *in nature* EO were verified, confirming the successful EO encapsulation within the wall materials. However, the peak located at  $3,460\text{ cm}^{-1}$  was more intense in the membrane spectrum. This fact may be explained due to exposure of the freeze-dried sample to the high humidity. For this reason, the reactions of water molecules were directly monitored by detecting the O-H stretching bands of weakly H-bonded O-H of water.

The prepared colloidal systems presented high encapsulation efficiency of EO, and the values were found as follow: PUC<sub>100</sub> ( $92.2 \pm 0.5$  %), PUC<sub>250</sub> ( $92.9 \pm 0.5$ %) and PUC<sub>500</sub> ( $94.7 \pm 0.5$ %). When the absolute concentration of EO increased from  $100\mu\text{g mL}^{-1}$  to  $500\mu\text{g mL}^{-1}$  (maintaining the gelatin concentration), the EE values increased about 2.6%. Thus, the various EO concentration have no significant impact on the EE.

The encapsulation of the rosemary EO in polycaprolactone (PCL)-based nano capsules synthesized by the nano precipitation method was previously reported [20]. The authors also observed encapsulation efficiency higher than 90%. Another study reported the encapsulation of the EO from *Piper aduncum* and *Piper hispidinervum* in PCL/gelatin nanoparticles [21]. The developed loaded nanoparticles also presented high encapsulation efficiency: the EE was observed higher than 80% when  $1,000\mu\text{g mL}^{-1}$  of EO was encapsulated.

### 3.2. Zeta Potential

The zeta potential is one of the most important factors of nanoparticles stability: the higher its value, the greater the nanoparticles repulsion, which avoids aggregation / agglomeration [22]. The zeta potential of the unloaded nanoparticles was found to be  $(-16 \pm 3)$  mV. For loaded nanoparticles, the zeta potentials were found around  $(-37 \pm 3)$  mV,  $(-39 \pm 3)$  mV, and  $(-39 \pm 3)$  mV for PUC<sub>100</sub>, PUC<sub>250</sub> and PUC<sub>500</sub> samples, respectively. The charges may be related to the compounds used to produce the nanoparticles and to rearrangements among the EO constituents. The zeta potential values were greater (in module) after the EO encapsulation, indicating that the presence of their constituents probably results in better stabilization of the nanoparticles charges due to intermolecular interactions. Furthermore, the zeta potential values for all solutions indicated good stability since all are larger, in modulus, than  $-30\text{mV}$ . In this case, the repulsive forces tend to form possible aggregations of the system due to

the collisions with other nanoparticles, never reaching the isoelectric point.

### 3.3. AFM and SEM Analyses

Nanoparticles size constituting the colloidal systems was estimated using the AFM technique and revealed that the loaded nanoparticles are spherical and well dispersed, as shown in Figure 2. The average size of the loaded nanoparticles is dependent on the EO concentration. The average size was observed around  $62 (\pm 2)$  nm,  $160 (\pm 4)$  nm and  $303 (\pm 4)$  nm for the samples PUC<sub>100</sub>, PUC<sub>250</sub> and PUC<sub>500</sub>, respectively. An increase of 80% was observed in the average nanoparticle size comparing the lowest ( $100\mu\text{g mL}^{-1}$ ) and the larger ( $500\mu\text{g mL}^{-1}$ ) absolute concentration of EO. The span values were found below 0.46 for all samples, as shown in Figure 3.

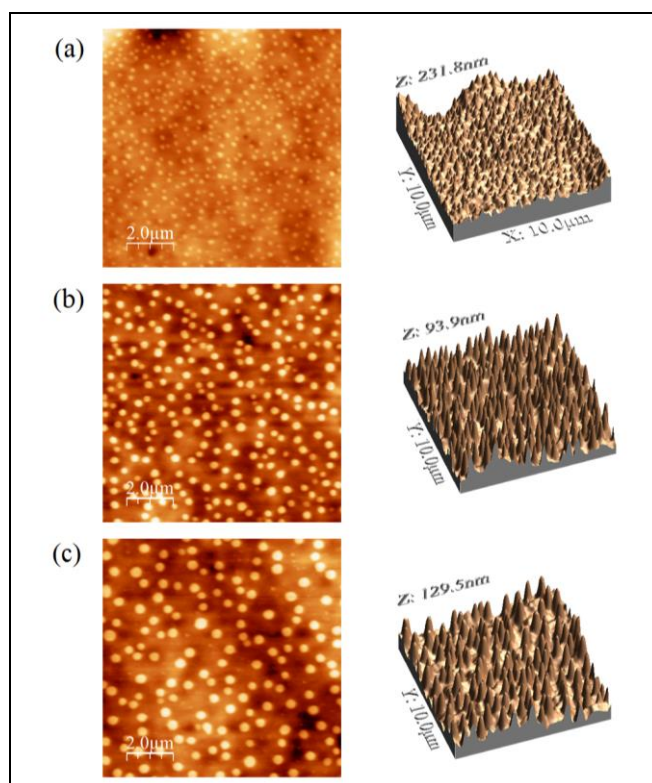


Fig 2: Nanoparticles from colloidal system visualized by AFM technique.

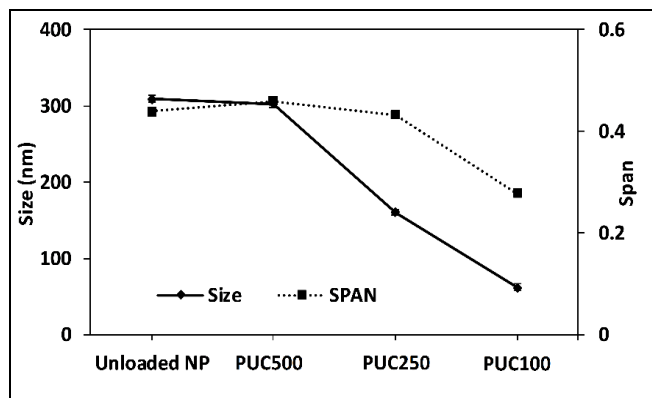
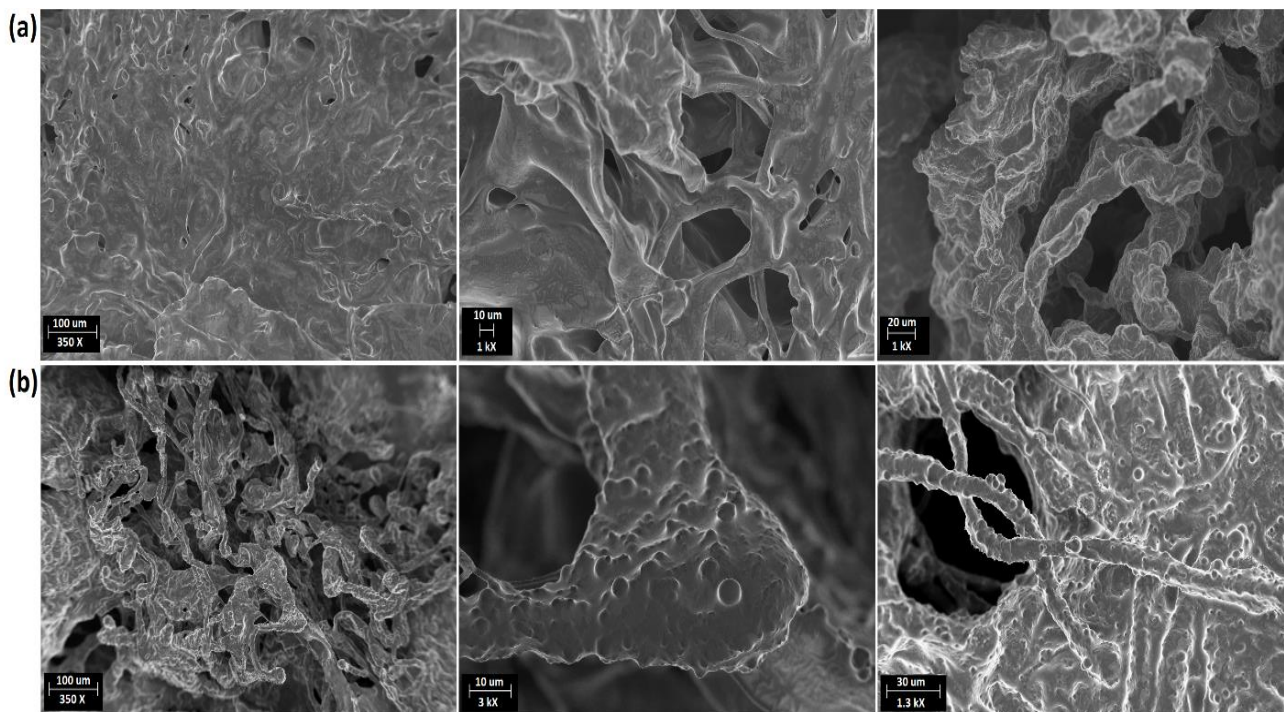


Fig 3: Nanoparticles size and span values of the colloidal systems.

Figure 4: shows the SEM images of the PCL/gelatin-based microparticles in the membrane form. The membranes containing the unloaded and loaded nanoparticles are shown in Figure 4a and 4b, respectively.



**Fig 4:** SEM images of the PCL/gelatin-based particles in the membrane form (a) containing the unloaded and (b) loaded nanoparticles.

The images revealed that the membranes are composed of fibers of different thicknesses. The wide distribution of the nanoparticles in the membrane form made it difficult to obtain their size distribution. However, the freeze-drying process promoted an agglomeration of nanoparticles, resulting in particles of micrometric sizes.

### 3.4. Controlled Release of Essential Oil

Figure 5 shows the controlled release behavior of the EO loaded in the PCL/gelatin-based nanoparticles colloidal systems. Different absolute concentrations of EO ( $100 \mu\text{g mL}^{-1}$ ,  $250 \mu\text{g mL}^{-1}$  or  $500 \mu\text{g mL}^{-1}$ ) were encapsulated.

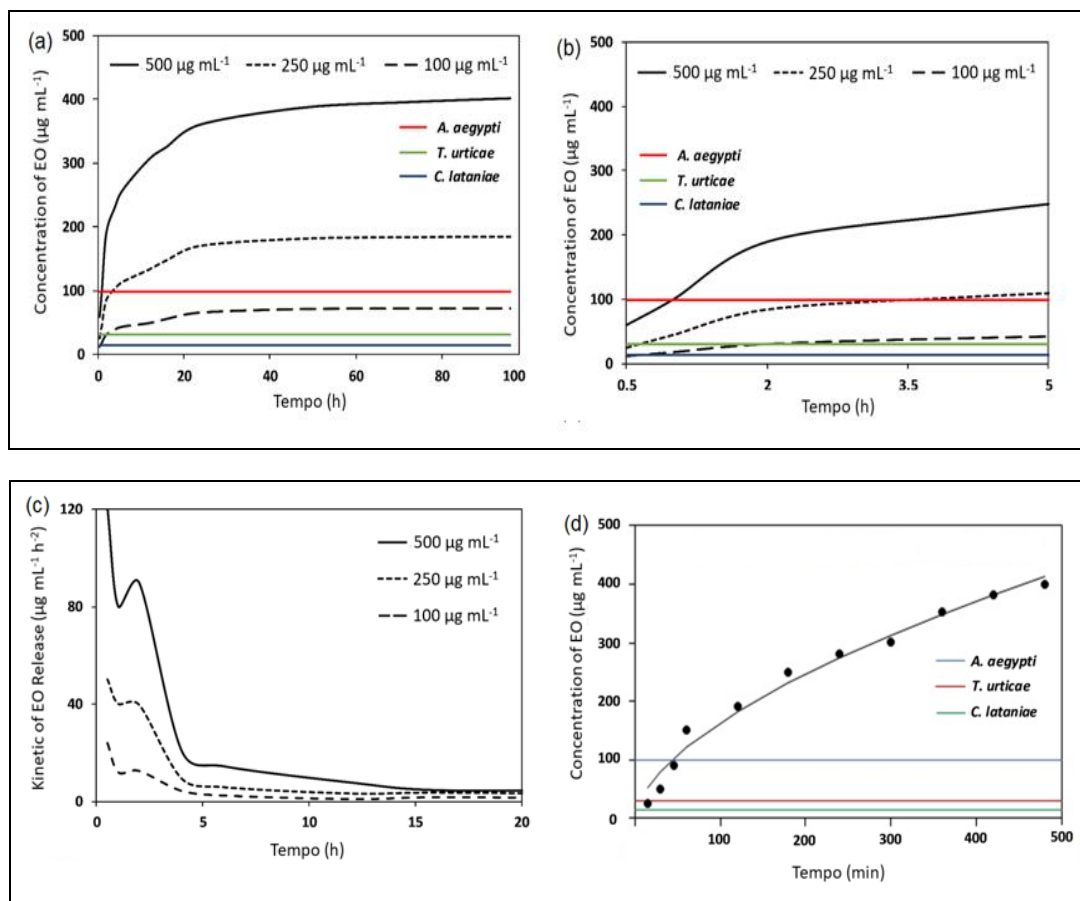


**Fig 5:**(a-b) curves of the released concentration of EO as a function of time for all colloidal systems; (c) kinetic curves of EO release derived from the obtained release curves and (d) curve of the released concentration of EO as a function of time for the membrane-based PCL/gelatin particles.

Figure 5a shows the curves of the released concentration of EO as a function of time for all colloidal systems. The horizontal lines represent the lethal dosages (LD<sub>50</sub>) needed to control the pests *A. aegypti*, *T. urticae* and *C. lataniae*, which were obtained from previous work [4]. The controlled release test was evaluated up to 100 h. Figure 5b shows that the LD<sub>50</sub> for the control of *T. urticae* and *C. lataniae* were reached in a few minutes of release and, after 1h, the LD<sub>50</sub> of *A. aegypti* was then achieved. After reaching the LD<sub>50</sub> of these three evaluated pests, the systems maintained their release of EO over time above the LD<sub>50</sub> values. Each system released its maximum concentration of EO up to 100 h. The absolute encapsulated concentration of 250 µg mL<sup>-1</sup> showed to be efficient to control all three tested pests. However, the LD<sub>50</sub> for the control of *A. aegypti* was reached only after 3.5 h. Figure 5c shows the kinetic curves of EO release, which were derived from the obtained release curves (Figure 5a). Two peaks of pronounced kinetic of EO release were observed. The first peak was observed after around 40 min of release, and the second after 2 h. The kinetics of release did not show any further expressive peak after 5 h of EO release, remaining almost constant over time.

Table 1 shows the t<sub>20%</sub> and t<sub>50%</sub> values, which correspond to the time at which 20% and 50% of the retained EO were released, respectively. The t<sub>20%</sub> was smaller for the colloidal systems containing larger absolute concentration of encapsulated EO: the system containing the encapsulated absolute concentration of 500 µg mL<sup>-1</sup> released 20% of this EO after 1 h. On the other hand, the systems containing the encapsulated absolute concentrations of 250 µg mL<sup>-1</sup> and 100 µg mL<sup>-1</sup> released 20% of EO after 1.8 h. The t<sub>50%</sub> was also smaller for the system containing larger absolute concentration of encapsulated EO: the system containing encapsulated absolute concentrations of 500 µg mL<sup>-1</sup>, 250 µg mL<sup>-1</sup> and 100 µg mL<sup>-1</sup> released 50% of this EO after, respectively, 4.7 h, 8.2 h and 12.5 h.

**Table 1:** t<sub>20%</sub> and t<sub>50%</sub> for different concentrations of encapsulated EO in the colloidal systems and membrane.

Colloidal Systems			
t (hours)	500 µg mL <sup>-1</sup>	250 µg mL <sup>-1</sup>	100 µg mL <sup>-1</sup>
t <sub>20%(h)</sub>	1.0	1.9	1.8
t <sub>50%(h)</sub>	4.7	8.2	12.5
Membrane System			
t <sub>20%(h)</sub>	0.4	-	-
t <sub>50%(h)</sub>	2.4	-	-

Figure 5d shows the curve of the released concentration of EO as a function of time for the membrane-based PCL/gelatin particles. The release of EO was faster than that observed for the colloidal systems. The membrane hydration during the controlled release assay may have promoted such faster release of EO. On the other hand, as observed in SEM images, the particles dispersed in the membrane are larger (micrometric) than those observed in the colloidal systems. For this reason, the encapsulated EO volume per particle may become larger, reducing the time of release. The maximum EO concentration released (around 400 µg mL<sup>-1</sup>) was reached in 500 min. All LD<sub>50</sub> were reached during the release process. In contrast, the LD<sub>50</sub> for the control of *T. urticae* and *C. lataniae* were reached in the first minutes of release. The LD<sub>50</sub> for *A. aegypti* was reached after 40 min. The t<sub>20%</sub> and t<sub>50%</sub> (Table 1) were found around, respectively, 0.4 h and 2.4 h, which are approximately the half of the values obtained for

the colloidal system containing the EO absolute concentration of 500 µg mL<sup>-1</sup>.

For all systems the release of 100% of the encapsulated EO was not observed and can be explained by the strong interaction between the EO and the wall materials. Other encapsulation studies [15] also reported the partial release of encapsulated bioactive compounds.

The release kinetic of the EO was analyzed from cumulative release data over time by fitting the data following the equation [(M<sub>t</sub>/M<sub>∞</sub>) = kt<sup>n</sup>] [11]. M<sub>t</sub>/M<sub>∞</sub> represents the fractional bioactive compound released at time t, n is a diffusion parameter characterizing the release mechanism, and k is a constant characteristic of the bioactive-polymer system [11,23,24]. Using the least-squares procedure, the k and n values were estimated and shown in Table 2. If n = 0.5, the bioactive diffuses and releases from the polymer matrix following quasi-Fickian diffusion. For n < 0.5, anomalous or non-Fickian type diffusion occurs. If n = 1, a completely non-Fickian case II or zero-order release kinetics is operative. Intermediary values between 0.5 and 1.0 are attributed to the anomalous type transport.

**Table 2:** Coefficients of Higuchi and Korsmeyer-Peppas models for kinetics of EO release

Colloidal Systems				
Model	Coeff.	500 µg mL <sup>-1</sup>	250 µg mL <sup>-1</sup>	100 µg mL <sup>-1</sup>
Higuchi	k	14.75	13.96	13.43
	R <sup>2</sup>	0.77	0.79	0.82
	k	30.84	27.21	25.73
Korsmeyer-Peppas	n	0.23	0.24	0.25
	R <sup>2</sup>	0.94	0.95	0.96
Membrane System				
	k	10.79	-	-
Korsmeyer-Peppas	n	0.59	-	-
	R <sup>2</sup>	0.98	-	-

The Korsmeyer-Peppas model better adjusted the controlled release data of the colloidal systems (with higher average R<sup>2</sup> value). For all colloidal systems n < 0.5, confirming the anomalous or non-Fickian type diffusion mechanism of the EO to the solvent medium [25]. For this reason, the rapid release of EO observed in the first minutes may be explained by the bulk erosion of the wall materials [26]. Mass erosion of biodegradable polymers is a chemical process involving the hydrolysis of the polymer with the presence of water into the polymer matrix [27]. Bulk erosion is common in polymer nanoparticles containing ester, ether and amine groups such as gelatin [13].

The Korsmeyer-Peppas model also better adjusted the controlled release data of the membrane system, with n > 0.5, confirming the anomalous type transport. This result can explain the faster EO release observed in the membrane-based PCL/gelatin particles. In particular, the use of membrane system for the encapsulation of this EO could ensure greater biological activity and efficiency in the field, since the freeze-dried colloidal system to form membranes could result in a material with greater stability, ease of storage and longer shelf life, resulting in higher quality, and greater economic value of agricultural products.

#### 4. Conclusions

The EO from *L. puchury-major* could be encapsulated successfully within PCL/gelatin particles. The FTIR spectra of the colloidal system and membrane containing particles loaded with EO confirmed its successful encapsulation. The

EE of the essential oil was higher than 90% for all colloidal systems. The zeta potential indicated that the encapsulation of EO resulted in better stabilization of the nanoparticle charges of the colloidal systems probably due to intermolecular interactions. The nanoparticles size of the colloidal system revealed that the loaded nanoparticles are spherical and well dispersed. However, their average size was dependent on the EO concentration. The membrane images revealed that the lyophilization process promoted an agglomeration of nanoparticles, resulting in particles in micrometric sizes. All colloid systems released their EO efficiently up to 100 h. The absolute encapsulated concentration of 250  $\mu\text{g mL}^{-1}$  showed to be efficient to combat all three tested pests. However, the release of EO from the membrane was faster than that observed for the colloidal systems probably due its hydration during the controlled release assay. The maximum EO concentration released from membrane was reached in 500 min. All LD<sub>50</sub> were reached during the release process. The freeze-dried colloidal system to form membranes could result in a material with greater stability and economic value of agricultural products. Furthermore, colloidal systems or membrane-based PCL/gelatin particles containing the EO from *L. puchury-major* was shown to be feasible as a sustainable alternative to combat the tested pests due to their encapsulation efficiency, biodegradability, adequate controlled release that reaches specific lethal dosages, and abundance of these plant species in the Amazon region.

## 5. Acknowledgment

The authors thank *Conselho Nacional de Desenvolvimento Científico e Tecnológico – CNPq (MCTI/CT-AGRONEGÓCIO/CT-AMAZÔNIA, grant number 403496/2013-6; Universal, grant number 401508/2016-1)* for the financial support.

## 6. References

1. Digilio MC, Mancini E, Voto E, Feo V De. Insecticide activity of Mediterranean essential oils. *Journal of Plant Interactions*. 2008; 3:17-23.
2. Sampson BJ, Tabanca N, Kirimer N, Demirci B, Baser KHC, Khan IA *et al*. Insecticidal activity of 23 essential oils and their major compounds against adult *Lipaphis pseudobrassicae* (Davis) (Aphididae: Homoptera). *Pest Management Science*. 2005; 61:1122-1128.
3. Mar JM, Silva LS, Azevedo SG, França LP, Goes AFF, Santos AL dos, *et al*. *Lippia organoides* essential oil: An efficient alternative to control *Aedes aegypti*, *Tetranychus urticae* and *Cerataphis lataniae*. *Industrial Crops and Products*. 2018; 111:292-297.
4. Azevedo SG, Mar JM, Silva LS da, França LP, Machado MB, Tadei WP *et al*. Bioactivity of *Licaria puchury-major* essential oil against *Aedes aegypti*, *Tetranychus urticae* and *Cerataphis lataniae*. *Records of Natural Products*. 2018; 12:229-238.
5. Benelli G, Canale A, Conti B. Eco-friendly control strategies against the Asian tiger mosquito, *Aedes albopictus* (Diptera: Culicidae): Repellency and toxic activity of plant essential oils and extracts. *Pharmacology online*. 2014; 1:44-51.
6. Campolo O, Romeo FV, Algeri GM, Laudani F, Malacrinó A, Timpanaro N *et al*. Larvicidal effects of four citrus peel essential oils against the arbovirus vector *Aedes albopictus* (Diptera: Culicidae). *Journal of Economic Entomology*. 2016; 109:360-365.
7. Maji TK, Hussain MR. Microencapsulation of *Zanthoxylum limonella* oil (ZLO) in genipin crosslinked chitosan-gelatin complex for mosquito repellent application. *Journal of Applied Polymer Science*. 2009; 111:779-785.
8. Perlatti B, Souza Bergo PL de, Fernandes da Silva MF das G, Batista J, Rossi M. Polymeric nanoparticle-based insecticides: A controlled release purpose for agrochemicals. *Insecticide - Development of safer and more effective technology*. Intech Open, 2013.
9. Papanikolaou NE, Kalaitzaki A, Karamaouna F, Michaelakis A, Papadimitriou V, Dourtoglou V *et al*. Nano-formulation enhances insecticidal activity of natural pyrethrins against *Aphis gossypii* (Hemiptera: Aphididae) and retains their harmless effect to non-target predators. *Environmental Science and Pollution Research*. 2017; 25:10243-10249.
10. Pfister G, Bahadir M, Korte F. Release characteristics of herbicides from Ca alginate gel formulations. *Journal of Controlled Release*. 1986; 3:229-233.
11. Naidu BVK, Paulson AT. A New Method for the Preparation of Gelatin Nanoparticles: Encapsulation and Drug Release Characteristics B. *Journal of Applied Polymer Science*. 2011; 121:3495-3500.
12. Ghasemishahrestani Z, Mehta M, Darne P, Yadav A, Ranade S. Tunable synthesis of gelatin nanoparticles employing sophorolipid and plant extract, a promising drug carrier. *World Journal of Pharmacy and Pharmaceutical Sciences*. 2015; 4:1365-1381.
13. Young S, Wong M, Tabata Y, Mikos AG. Gelatin as a delivery vehicle for the controlled release of bioactive molecules. *Journal of Controlled Release*. 2005; 109:256-274.
14. Gubler DJ. Prevention and control of *Aedes aegypti*-borne diseases: Lesson learned from past successes and failures. *Asia-Pacific Journal of Molecular Biology and Biotechnology*. 2013; 19:111-114.
15. Flechtmann CHW. Rediscovery of *Tetranychus abacae* Baker & Pritchard, Additional description and notes on South American spider mites (Acari, Prostigmata, Tetranychidae). *Revista Brasileira de Zoologia*. 1996; 13:569-578.
16. Souza LA, Lemos WP. Prospecção de insetos associados ao açazeiro (*Euterpe oleracea* Mart.) em viveiro e proposições de controle. *Revista de Ciências Agrárias*. 2004; 42:231-241.
17. Schneider CA, Rasband WS, Eliceiri KW. NIH Image to ImageJ: 25 years of image analysis. *Nature Methods Nature Publishing Group*. 2012; 9:671-675.
18. Kalsi PS. Spectroscopy of organic compounds. 6th ed. New Delhi: New Age International, 2005.
19. Yakimets I, Wellner N, Smith AC, Wilson RH, Farhat I, Mitchell J. Mechanical properties with respect to water content of gelatin films in glassy state. *Polymer*. 2005; 46:12577-12585.
20. Ephrem E, Greige-Gerges H, Fessi H, Charcosset C. Optimisation of rosemary oil encapsulation in polycaprolactone and scale-up of the process. *Journal of Microencapsulation*. 2014; 31:746-753.
21. Silva LS, Mar JM, Azevedo SG, Rabelo MS, Bezerra JA, Campolo PH *et al*. Encapsulation of *Piper aduncum* and *Piper hispidinervum* essential oils in gelatin nanoparticles: a possible sustainable control tool of *Aedes aegypti*, *Tetranychus urticae* and *Cerataphis lataniae*. *Journal of the Science of Food and Agriculture*. 2018; 99:685-695.

22. Honary S, Zahir F. Effect of zeta potential on the properties of nano-drug delivery systems - A review (Part 2). *Tropical Journal of Pharmaceutical Research*. 2013; 12:265-273.
23. Buntner B, Nowak M, Kasperczyk J, Ryba M, Grieb P, Walski M *et al*. The application of microspheres from the copolymers of lactide and  $\epsilon$ -caprolactone to the controlled release of steroids. *Journal of Controlled Release*. 1998; 56:159-167.
24. Ritger PL, Peppas NA. A simple equation for description of solute release II. Fickian and anomalous release from swellable devices. *Journal of Controlled Release*. 1987; 5:37-42.
25. Siepmann J, Peppas NA. Higuchi equation: Derivation, applications, use and misuse. *International Journal of Pharmaceutics*. 2011; 418:6-12.
26. Burkersroda FV, Schedl L, Göpferich A. Why degradable polymers undergo surface erosion or bulk erosion. *Biomaterials*. 2002; 23:4221-4231.
27. Göpferich A. Polymer Bulk Erosion. *Macromolecules*. 1997; 30:2598-2604.